Molecular Crystals and Liquid Crystals

ISSN: 1542-1406 (Print) 1563-5287 (Online) Journal homepage: http://www.tandfonline.com/loi/gmcl20

The Effect of Plasticization on Conductivity and Other Properties of Starch/Chitosan Blend Biopolymer Electrolyte Incorporated with Ammonium Iodide

Y. M. Yusof, N. A. Majid, R. M. Kasmani, H. A. Illias & M. F. Z. Kadir

To cite this article: Y. M. Yusof, N. A. Majid, R. M. Kasmani, H. A. Illias & M. F. Z. Kadir (2014) The Effect of Plasticization on Conductivity and Other Properties of Starch/Chitosan Blend Biopolymer Electrolyte Incorporated with Ammonium Iodide, Molecular Crystals and Liquid Crystals, 603:1, 73-88, DOI: 10.1080/15421406.2014.966261

To link to this article: http://dx.doi.org/10.1080/15421406.2014.966261

Mol. Cryst. Liq. Cryst., Vol. 603: pp. 73–88, 2014

ISSN: 1542-1406 print/1563-5287 online
DOI: 10.1080/15421406.2014.966261

The Effect of Plasticization on Conductivity and Other Properties of Starch/Chitosan Blend Biopolymer Electrolyte Incorporated with Ammonium Iodide

Y. M. YUSOF,[1] N. A. MAJID,[2] R. M. KASMANI,[3] H. A. ILLIAS,[4] AND M. F. Z. KADIR[3,*]

[1]Institute of Graduate Studies, University of Malaya, Kuala Lumpur 50603, Malaysia
[2]Institute of Biological Sciences, Faculty of Science, University of Malaya, Kuala Lumpur 50603, Malaysia
[3]Centre for Foundation Studies in Science, University of Malaya, 50603, Kuala Lumpur, Malaysia
[4]Department of Electrical Engineering, Faculty of Engineering, University of Malaya, 50603, Kuala Lumpur, Malaysia

This work focuses on polymer electrolytes composed of a starch-chitosan blend host, ammonium iodide (NH_4I) and glycerol. Fourier transform infrared (FTIR) analysis confirms the interaction of starch-chitosan-NH_4I-glycerol. The highest room temperature conductivity is $(1.28 \pm 0.07) \times 10^{-3}$ S cm^{-1}, obtained by a sample containing 30 wt% glycerol. Dielectric studies showed that the electrolytes obeyed non-Debye behavior. The total ionic transference number for the 30 wt% glycerol sample was 0.991, and the conduction mechanism for this sample followed the quantum mechanical tunneling (QMT) model. Linear sweep voltammetry (LSV) showed that this sample was electrochemically stable up to 1.90 V. The highest conducting sample was used in the fabrication of an electrical double layer capacitor (EDLC) cell.

Keywords Polymer electrolyte; conductivity; starch-chitosan blend; ammonium iodide; EDLC

Introduction

Solid polymer electrolyte (SPE) based ionic conductors have been investigated widely because they offer advantages such as ease of fabrication, good shelf life and good mechanical properties [1]. Various polymers have been investigated including chitosan [2], methyl cellulose (MC) [3], starch [4], polyethylene oxide (PEO) [5] and polyvinyl alcohol (PVA) [6]. Polymers obtained from natural polymers such as starch, cellulose and chitosan have attracted attention due to their biodegradable, renewable and sustainable properties [7–10].

*Address correspondence to M. F. Z. Kadir, Centre for Foundation Studies in Science, University of Malaya, 50603 Kuala Lumpur, Malaysia; E-mail: mfzkadir@um.edu.my

Color versions of one or more of the figures in the article can be found online at www.tandfonline.com/gmcl.

Among the natural biopolymers, starch has received the most attention because of its low cost, availability, and total degradation after usage [11]. However, there are some major drawbacks of these films including poor mechanical properties and a strong hydrophilic nature [12].

Various methods have been applied in order to improve the mechanical properties of the polymer films. Blending two or more polymers is one of the easiest and cheapest techniques where the physical properties can be controlled. Furthermore, it can also leads towards the enhancement of the ionic conductivity [13]. When chitosan was dissolved in aqueous solutions of some organic and inorganic acids, a cationic polymer is formed because of protonation of amino groups on the C-2 position of the pyranose ring [14]. Chitosan consists of a large number of amino and hydroxyl groups. These two functional groups provide several possibilities for grafting of desirable bioactive groups [15, 16]. Since chitosan is non-toxic and biocompatible with the human physiological system, it has been investigated as a biomaterial in the fields such as biomedicine, pharmacology and biotechnology [17, 18]. Bourtoom and Chinnan [19] and Zhai et al. [20] reported that when starch was blended with chitosan, the mechanical strength of the blend increased and the crystallinity was suppressed. Starch-chitosan blends exhibit good film-forming properties due to the presence of a high density of amino groups and hydroxyl groups with inter and intra molecular hydrogen bonding [21]. Khiar and Arof [22] reported that the ionic conductivity of 2.83×10^{-5} S cm^{-1} at room temperature for starch doped with ammonium nitrate (NH_4NO_3) increased to 3.89×10^{-5} S cm^{-1} by blending starch and chitosan [23]. Buraidah and Arof [24] also reported that the conductivity of 55 wt% chitosan-45 wt% NH_4I increased from 3.73×10^{-7} S cm^{-1} to 1.77×10^{-6} S cm^{-1} when blended with PVA.

In the present work, a starch-chitosan blend was doped with NH_4I salt and further plasticized with glycerol. Ammonium iodide was chosen in this work since it possesses a low lattice energy for fast ion transportation [24]. From our previous work, the sample that consisted of 40 wt% NH_4I attained the highest conductivity value of 3.04×10^{-4} S cm^{-1} [25]. The ionic transportation is believed to become faster when a high dielectric constant plasticizer is added and in this work, glycerol has been used. The effects of the glycerol towards the conductivity increment and other electrical properties are analyzed. The highest conducting sample in this work was applied in the fabrication of an electrical double layer capacitor (EDLC).

Experimental Methods

Preparation of Electrolytes

0.80 g of corn starch (Brown and Polson) was dissolved in 100 ml of 1% acetic acid (SYSTERM) at 80°C for 20 minutes. After the solution cooled to room temperature, 0.20 g of chitosan [viscosity: 800–2000 cP; 1 wt% in 1% acetic acid (25°C), Sigma-Aldrich] was added. 40 wt% of ammonium iodide, NH_4I (HmbG) was added to the 4:1 starch-chitosan blend solution and stirred until homogeneous solution was obtained. Different amounts of glycerol (SYSTERM) were added to the starch-chitosan-NH_4I electrolyte solution and stirred until complete dissolution. All solutions were cast on plastic Petri dishes and left to dry at room temperature. The dry films were kept in a glass desiccator filled with silica gel desiccants for further drying. The compositions and designations of the electrolytes are presented in Table 1.

Table 1. Composition and designation of electrolytes

Starch: chitosan: NH_4I: glycerol composition (wt%)	Designation
48: 12: 40: 0	A4 [25]
43: 11: 36: 10	B1
38: 10: 32: 20	B2
34: 8: 28: 30	B3
29: 7: 24: 40	B4
24: 6: 20: 50	B5

Electrolyte Characterization

Fourier transform infrared (FTIR) spectroscopy studies were recorded using the Spotlight 400 Perkin-Elmer spectrometer in the wavenumber range of 400–4000 cm^{-1}. Impedance measurements were conducted using HIOKI 3532-50 LCR HiTESTER from room temperature to 348 K in the frequency range of 50 Hz to 5 MHz. The conductivity of the electrolyte was calculated using:

$$\sigma = \frac{d}{R_b A} \tag{1}$$

where d is the thickness of the electrolyte, R_b is the bulk resistance and A is the electrode–electrolyte contact area. The electrolytes were sandwiched between two stainless steel electrodes of a conductivity holder. The value of R_b was determined from the Cole-Cole plot obtained from the impedance measurements. The total ionic transference number has been evaluated by a polarization technique. A d.c. voltage source was used at a constant dc potential of 0.80 V to polarize the cell. Stainless steel (SS) blocking electrodes were used to sandwich the highest conducting polymer electrolytes with cell configuration SS/30 wt% glycerol (B3) sample/SS at room temperature. Linear sweep voltammetry (LSV) measurement was conducted employing a 3-electrode configuration where stainless steel electrodes were employed as working, counter and reference electrodes. This electrochemical stability window was measured using Digi-Ivy DY2300 potentiostat at a scan rate of 1 mV s^{-1} in a potential range of 0 V to 2.50 V. LSV measurement was conducted at room temperature.

Preparation of Electrodes

The EDLC electrodes were prepared by mixing 13 g activated carbon (RP20, manufactured by Kuraray, Japan), 2 g poly(vinylidene fluoride) (PVdF) and 1 g carbon black (Super P) in 60 ml N-methylpyrrolidone (NMP) (EMPLURA). The mixture was stirred until a homogeneous slurry was obtained. The slurry was then spread on an aluminium foil using the doctor blade method and heated at 60°C. The dry electrodes were kept in a desiccator filled with silica gel desiccants for further drying.

EDLC Fabrication and Characterization

The performance of EDLC was characterized using cyclic voltammetry (CV) and charge-discharge cycling at constant current. The highest conducting sample was sandwiched between two carbon electrodes using perspex plates. CV was carried out at room temperature

using a Digi-IVY DY2300 potentiostat between 0 to 0.85 V at different scan rates. The galvanostatic charge-discharge characteristics of the EDLC were carried out using Neware battery cycler in a voltage range between 0 to 0.85 V at a constant current density of 0.04 mA cm^{-2}.

Results and Discussion

FTIR Studies

FTIR is a direct method to distinguish molecular interactions by monitoring the band shifts of certain functional groups [26]. Fig. 1(a) depicts the FTIR spectra of selected samples for the system in the region of 3100–3600 cm^{-1}. The hydroxyl band in the spectrum of A4 sample appears at 3338 cm^{-1} in Fig. 1(a). (i) This peak has shifted to lower wavenumbers, Fig. 1(a) (ii)–(vi), for the sample containing different amounts of glycerol, which implied that the addition of glycerol promotes the hydrogen bonding interactions between the electrolytes components. According to Liu et al. [26], when the glycerol concentration in the matrix is increased, more OH groups are available for starch-glycerol and/or chitosan-glycerol interactions. They reported that the hydroxyl band has shifted from 3339.57 cm^{-1} to 3336.82 cm^{-1} in starch-chitosan film containing 5 wt% and 10 wt% of glycerol, respectively.

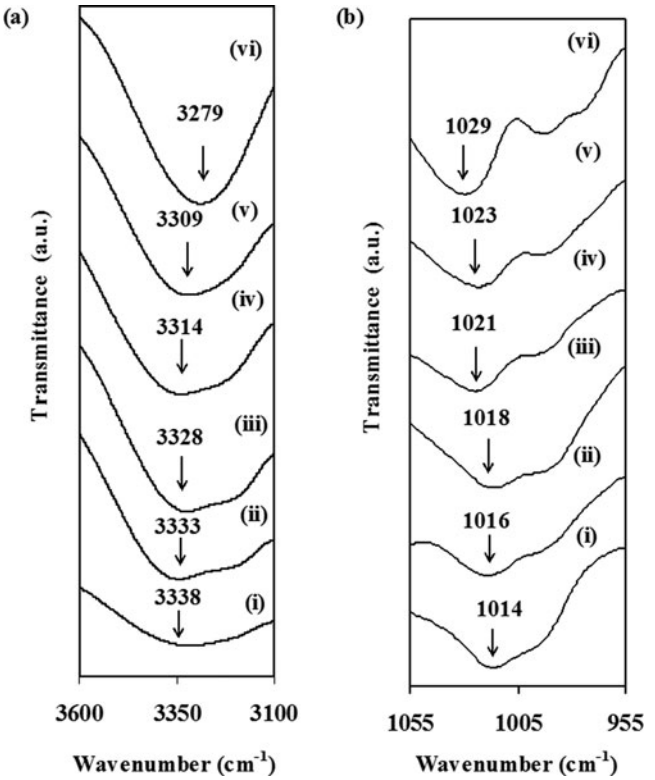

Figure 1. (a) FTIR spectra for A4 (i), B1 (ii), B2 (iii), B3 (iv), B4 (v) and pure glycerol (vi) in the region of 3100–3600 cm^{-1}. (b) FTIR spectra for A4 (i), B1 (ii), B2 (iii), B3 (iv), B4 (v) and pure glycerol (vi) in the region of 955–1055 cm^{-1}.

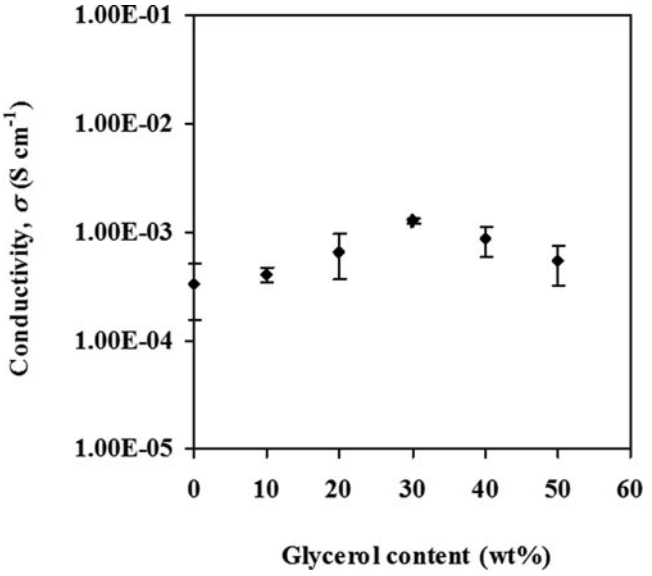

Figure 2. Effect of glycerol content on conductivity of the electrolytes at room temperature.

Figure 1(b) shows the FTIR spectra of selected samples for the system in the region of 955–1055 cm^{-1}. The peak observed at 1014 cm^{-1} in the spectrum of the A4 sample, Fig. 1(b) (i), has shifted to 1016 cm^{-1} in the spectrum of B1, Fig. 1(b) (ii) and further increases to higher wavenumbers with the increment of glycerol content, Fig. 1(b) (iii–vi). This can be associated with the amorphous characteristic of the material and also C—O—H bond vibration or solvation [27]. As the glycerol concentration increases, Bergo [28] reported that the peak observed at 1011.8 cm^{-1} in the spectrum of starch film without glycerol shifted to higher wavenumbers.

Conductivity Studies

Figure 2 represents the variation of room temperature conductivity as a function of glycerol concentration. The conductivity value of glycerol free film increased from $(3.04 \pm 0.32) \times 10^{-4}$ S cm^{-1} to a maximum value of $(1.28 \pm 0.07) \times 10^{-3}$ S cm^{-1} with 30 wt% of glycerol (i.e. B3 sample). This is because glycerol possesses a high dielectric constant which can weaken the Coulombic force between cation and anion of the salt hence more undissociated salt becomes free mobile ions [29]. Furthermore, the addition of plasticizer can create more pathways for ion conduction and can also increase ionic mobility [30, 31]. Shukur et al. [29] reported that when ethylene carbonate (EC) was added to the starch-chitosan-NH_4Br based electrolytes, the conductivity increased from 9.72×10^{-5} to 1.44×10^{-3} S cm^{-1}. From Fig. 2, it can be observed that further addition of glycerol decreased the conductivity due to the fact that the increase in glycerol content allows the formation of microcrystalline junctions which promote recrystallization of salt resulting in a drop in conductivity [28].

Dielectric Study

Study on the permittivity in polymer electrolyte films helps to understand the polarization effect at the electrode/electrolyte interface. Dielectric constant (ε_r) is a representative of

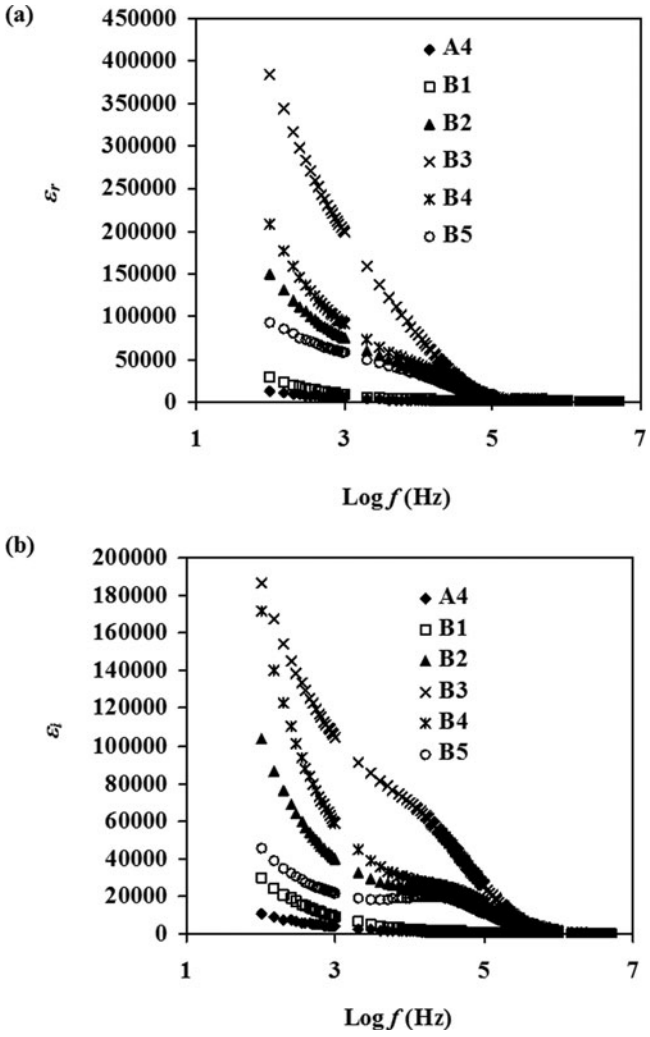

Figure 3. Frequency dependence of ε_r (a) and ε_i (b) at room temperature.

stored charge in a material while dielectric loss (ε_i) is a measure of energy losses to move ions and align dipoles when the polarity of electric field reverses rapidly [32]. From the impedance measurements, ε_r and ε_i can be calculated using equations:

$$\varepsilon_r = \frac{Z_i}{\omega C_o \left(Z_r^2 + Z_i^2\right)} \tag{2}$$

$$\varepsilon_i = \frac{Z_r}{\omega C_o \left(Z_r^2 + Z_i^2\right)} \tag{3}$$

Figure 3(a) and 3(b) depict the glycerol concentration dependence of dielectric constant and dielectric loss, respectively. Dispersion with a high value of ε_r and ε_i is observed in the low frequency region which is attributed to the dielectric polarization effect [33]. This phenomenon can be attributed to the build up of space charge near the electrode-electrolyte

interface which blocks the charge transport that does not permit charge transfer into the external circuit. An increase in dielectric constant will result in the increasing number of charge carriers in the space charge accumulation region and thus conductivity increases [34]. Due to its high dielectric constant, glycerol is able to dissociate more salt to cations and anions resulting in an increase in number density of mobile ions [30]. This indicates that the increase in conductivity is due to the increase in the concentration of mobile ions [22]. At high frequencies, these finite and reversible trapped ions accumulate at the interface of the electrode-electrolyte and become localized, which reduces the contribution of charge carriers towards the electrode [32]. The observed space charge regions with respect to the frequency can be explained through ion diffusion where the behaviour is generally known as the non-Debye type [22]. Shukur et al. [35] also reported that as more plasticizer was added, more undissociated salt become ions, hence increased the stored charge in the electrolyte. However, beyond the addition of 30 wt% of glycerol, ε_r was observed to decrease, which follows the same trend as their conductivity results.

Temperature-Dependent Conductivity

The variation of ionic conductivity with temperature for plasticized starch-chitosan-NH_4I system is shown in Fig. 4. The regression values, R^2 are almost 1 and therefore implies that the plots of log σ versus 1000/T are Arrhenian [1]. The activation energy, E_a of these polymer electrolytes is obtained from the slope of the plot based on equation:

$$\sigma = \sigma_0 \exp\left[\frac{-E_a}{kT}\right] \tag{4}$$

where σ_0 is a pre-exponential factor, E_a is the activation energy of conduction and k is Boltzmann constant. This conductivity trend has been interpreted by dielectric and FTIR results. The increase in conductivity can be attributed to the increase in number density

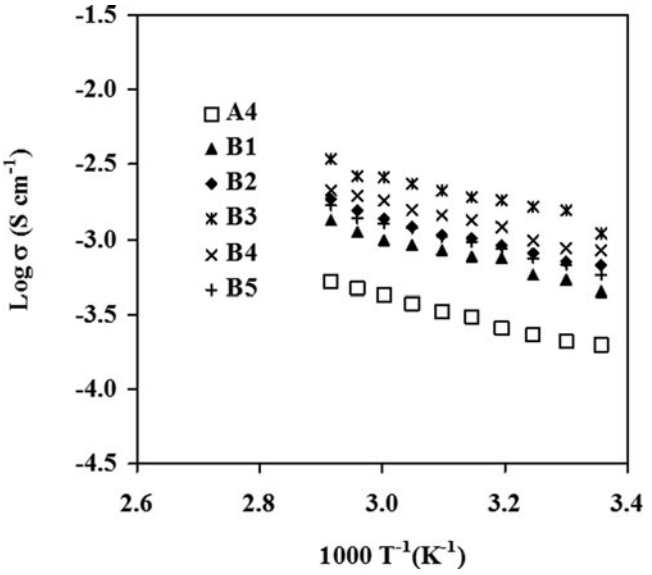

Figure 4. Conductivity of electrolytes at elevated temperatures.

Table 2. Transport parameters of electrolytes at room temperature

Sample	σ/S cm^{-1}	E_a/eV	τ /s	n/cm^{-3}	μ/cm^2 V^{-1} s^{-1}
A4 [25]	$(3.04 \pm 0.32) \times 10^{-4}$	0.201	1.68×10^{-13}	5.50×10^{18}	3.45×10^{-4}
B1	$(4.12 \pm 0.65) \times 10^{-4}$	0.198	1.69×10^{-13}	6.93×10^{18}	3.71×10^{-4}
B2	$(6.63 \pm 2.97) \times 10^{-4}$	0.193	1.71×10^{-13}	9.30×10^{18}	4.45×10^{-4}
B3	$(1.28 \pm 0.07) \times 10^{-3}$	0.182	1.76×10^{-13}	1.20×10^{19}	6.63×10^{-4}
B4	$(8.56 \pm 2.75) \times 10^{-4}$	0.190	1.72×10^{-13}	1.08×10^{19}	4.96×10^{-4}
B5	$(5.39 \pm 2.18) \times 10^{-4}$	0.194	1.70×10^{-13}	7.84×10^{18}	4.29×10^{-4}

and mobility of ions [36, 37]. The variation in activation energy values and conductivity indicates that the plasticizer promotes mobility of the ions by providing easier path ways. The above conduction characteristics show an enhancement in the conductivity and mobility of the ion, with a constant cationic transport number depends on plasticizer content which facilitates the dissociation of the salt [33].

The activation energy decreases with increasing conductivity as shown in Table 2. The highest conducting sample has the lowest activation energy of 0.182 eV. Since the ion transfer is greatly affected by the polymer segmental motion, an electrolyte with a lower value of E_a implies rapid ionic conduction and hence higher conductivity [1]. The correlations between conductivity and E_a of the chitosan-based polymer electrolyte reported by many researchers have shown similar behavior [30, 38, 39].

Transport Parameters

Table 2 lists the transport parameters at room temperature for complexes of starch-chitosan-NH_4I with various glycerol concentrations. To obtain the transport parameters in the present work, the Rice and Roth model [40] was employed. Ionic conductivity of an electrolyte depends on the number density and mobility of ions as expressed by the equation:

$$\sigma = nq\mu \tag{5}$$

where σ is ionic conductivity, n is number density, μ is mobility of mobile ions and q is electron charge. Number density of mobile ions is a very important parameter in understanding the transport properties of polymer electrolytes [38]. In this work the number density of mobile ions was calculated using the Rice and Roth [40] equation:

$$\sigma = \frac{2}{3}\left[\frac{(Ze)^2}{kTm}\right] nE_a\tau \exp\left(\frac{-E_a}{kT}\right) \tag{6}$$

where Z is the valency of conducting species, e is electron charge, m is mass of charge carrier, n is number density of ions and τ is travelling time of ions. The value of τ was obtained using the equation:

$$\tau = \frac{l}{v} \tag{7}$$

According to Khiar and Arof [22], l is the distance between two repeating unit of amylose fiber and taken to be around 10.40 Å which is used in the present study. Velocity

v of mobile ions is obtained using:

$$v = \sqrt{\frac{2E_a}{m}} \tag{8}$$

The ionic mobility μ was calculated using the value of n:

$$\mu = \frac{\sigma}{ne} \tag{9}$$

It is necessary to know the type of conducting ion since its mass must be known. Hashmi et al. [41] have proven that in polyethylene oxide, PEO complexed with ammonium perchlorate, NH_4ClO_4, the conducting species is H^+ ion which originates from the ammonium ion. Conduction of H^+ is explained by the Grotthuss mechanism. By virtue of their work, NH_4I is considered as the proton source in the present samples. Hence, the number density of mobile ions can be calculated from the Rice and Roth equation.

The values of n lies between 10^{18} and 10^{19} cm^{-3} and all μ values are in the range of 10^{-4} cm^2 V^{-1} s^{-1}. From Table 2, it can be concluded that the increasing conductivity value is influenced by the increasing mobility and number density of ions. The highest conducting sample for this system has the highest n and μ values of 1.20×10^{19} cm^{-3} and 6.63×10^{-4} cm^2 V^{-1} s^{-1}, respectively. Shukur et al. [35] reported that the n value of chitosan-PEO-NH_4NO_3 plasticized with 70 wt% ethylene carbonate (EC) electrolyte was 1.87×10^{19} cm^{-3} which is comparable with the present result. The addition of 40 and 50 wt% of glycerol decreased the number density and mobility of ions leading to conductivity decrement.

The Rice and Roth equation is based on the hypothesis that conducting ions can be thermally excited to propagate as free ions throughout the solid with the above velocity [42]. The change in conductivity with glycerol composition is due mainly to the change in free ion concentration. When the total amount of salt is the same, the change in n observed should be ascribed to the permittivity effect of the plasticizer. Due to the high dielectric constant of glycerol, increasing the glycerol content will increase the degree of ion dissociation, thus the conductivity is increased by the increase in the number of free ions [1]. The presence of glycerol in the electrolyte system produced more mobile ions and lowered the viscosity of the electrolyte that led to an increase in ionic mobility [43].

Conduction Mechanism

The ac conductivity, σ_{ac} can be obtained using:

$$\sigma_{ac} = \varepsilon_o \varepsilon_r \omega \tan\delta \tag{10}$$

Substituting $\varepsilon_r \tan\delta = \varepsilon_i$,

$$\sigma_{ac} = \varepsilon_o \varepsilon_i \omega \tag{11}$$

Generally, the phenomenon of σ_{ac} can be analyzed using the Jonscher's universal power law [44, 45]:

$$\sigma(\omega) = A\omega^s + \sigma_{dc} \tag{12}$$

where $\sigma(\omega)$ is the total conductivity, σ_{dc} is frequency independent dc conductivity, A is a temperature dependent parameter and s is the power law exponent. Since $\sigma_{ac} = A\omega^s$, the

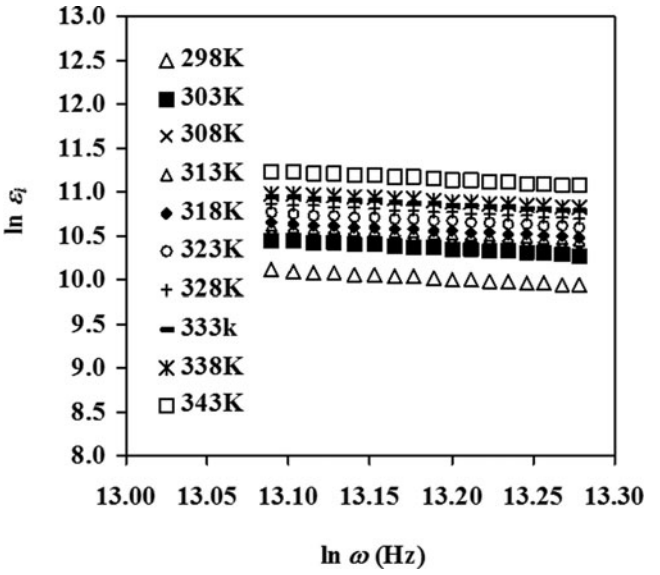

Figure 5. ln ε_i versus ln ω at different temperatures for the 30 wt% glycerol sample.

value of s can be evaluated from the following relation.

$$\ln \varepsilon_i = \ln \frac{A}{\varepsilon_o} + (s-1) \ln \omega \tag{13}$$

The value of the exponent s is obtained from the slope of the plot of ln ε_i against ln ω in Fig. 5. There are various reports which suggest the acceptable frequency range is in the high frequency region [30, 46]. This is because at high frequencies the electrode polarization occurs at minimum rate or does not occur at all [30]. In the present work, the acceptable frequency range was $13.09 \leq \ln \omega \leq 13.28$.

In the quantum mechanical tunneling (QMT) model, the exponent or index s is independent of temperature, which is shown by the small gradient [24, 47, 48], where in this work is 0.00008. From the observations on the behavior of the index s with temperature, Fig. 6, it can be inferred that QMT model is more applicable in explaining the conduction mechanism of this polymer electrolyte represented by the equation of $s = 0.00008T + 0.1059$. Psarras [44] has defined hopping as the displacement of a charge carrier from one site to another neighboring site and occurs not just by jumping over a potential barrier but can also be accompanied by quantum mechanical tunneling. The ions are able to tunnel through the potential barrier that exists between two possible complexation sites [49].

Ionic Tranference Number

The contribution of total ionic conductivity of the polymer electrolyte was determined by polarizing the blocking electrode cell configuration SS/B3 sample/SS by applying 0.80 V and monitoring the potentiostatic current as a function of time, as shown in Fig. 7. The transference numbers corresponding to ionic (t_{ion}) and electronic (t_{elec}) have been evaluated

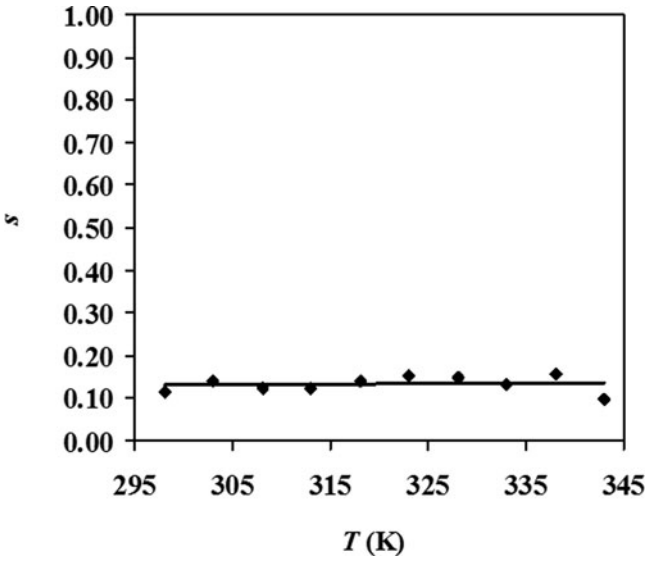

Figure 6. Plot of exponent (*s*) versus temperature (*T*) for the 30 wt% glycerol sample.

using Wagner's polarization technique using the equations:

$$t_{ion} = \frac{(I_i - I_f)}{I_i} \tag{14}$$

$$t_{elec} = \frac{I_f}{I_i} \tag{15}$$

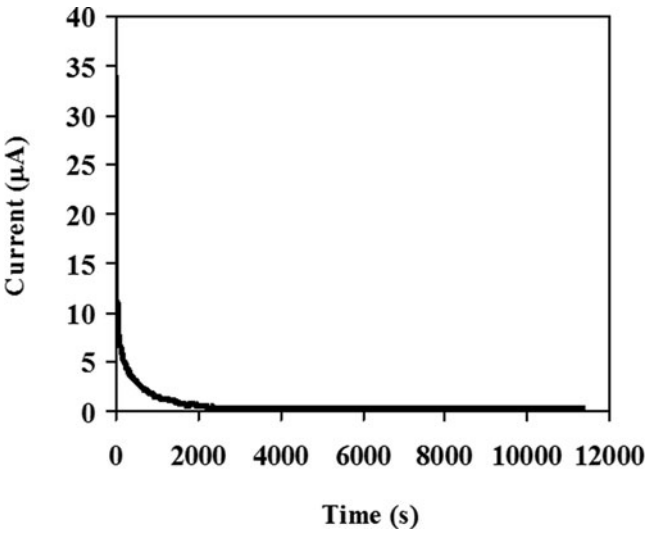

Figure 7. Current relaxation curve during dc polarization at an applied voltage of 0.8 V for blocking electrodes (SS/SPE/SS).

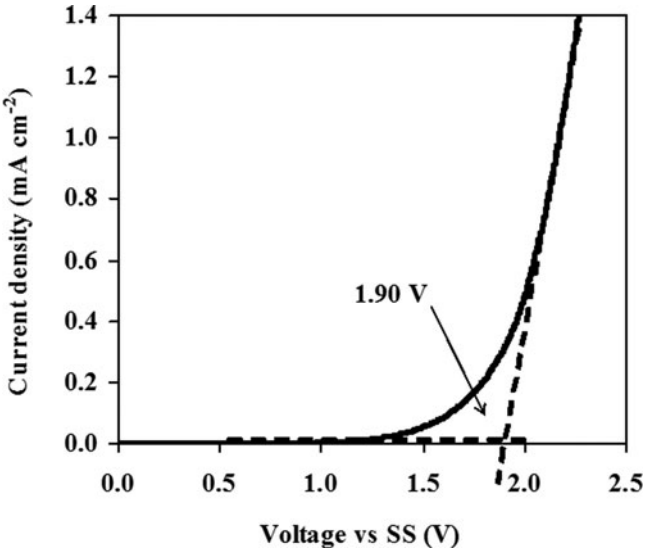

Figure 8. Linear sweep voltammetry curve for 30 wt% glycerol sample at room temperature.

where I_i is the initial current and I_f is the final residual current. From Fig. 7, the ionic transference number, t_{ion} and the electronic transference number, t_{elec} for the highest conducting sample was 0.991 and 0.009, respectively.

In Wagner's polarization technique, the DC current is monitored as a function of time on application of a fixed DC voltage across the sample with blocking and electrodes [50]. From the results we can see that the transference number for ions is much larger compared to the transference number for electrons. This suggests that in these polymer electrolytes, the charge transport is predominantly due to ions [51].

Linear Sweep Voltammetry

The electrochemical stability as well as the ability of membranes to endure the operating voltage of the fabricated device are important parameters for the characterization of prepared polymer electrolyte [52]. This parameter has been studied using LSV, and its corresponding voltammogram is shown in Fig. 8. Shukur et al. [35] have reported that the voltage breakdown for the chitosan-PEO based membrane containing NH_4NO_3 and EC is 1.75 V at ambient temperature. Kadir and Arof [53] reported that the voltage breakdown for PVA-chitosan based membrane containing NH_4NO_3 and EC plasticizer is $\sim$1.70 V at ambient temperature. From the LSV result, it can be observed that the decomposition voltage of the polymer electrolyte is around 1.90 V.

Fabrication and Characterization of EDLC

The CV of the EDLC was studied at various scan rates, as shown in Fig. 9. The figure shows the curves are nearly rectangular and without visible peaks due to redox reactions or electron transfer processes [54, 55]. This explains that the charge and discharge processes occur reversibly at the electrode-electrolyte interfaces [55]. The slight deviation from the rectangular shape of the CV curves was observed at higher scan rates is attributed to the

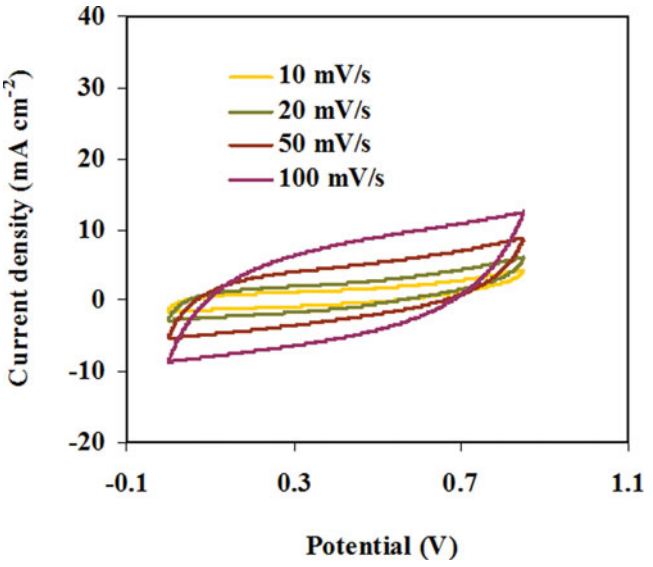

Figure 9. Plots of cyclic voltammogram of EDLC at various scan rates.

internal resistance and carbon porosity [53]. The current was delayed in reaching a constant value on reversible potential sweep, mainly at higher scan rates [54]. This voltammogram explains that EDLC is scan rate dependent which is a characteristic of capacitor cells.

The charge-discharge curves of EDLC at selected cycles using the highest conducting electrolyte are shown in Fig. 10. The EDLC was charged at room temperature from 0

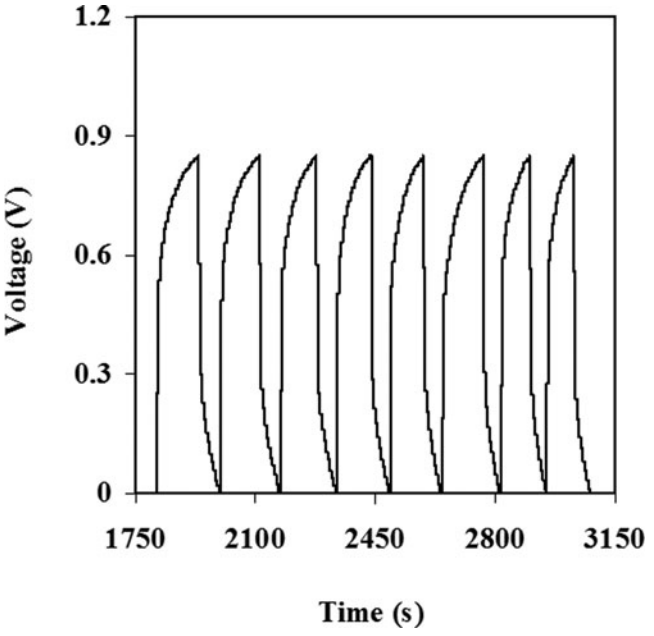

Figure 10. Charge-discharge profile of EDLC.

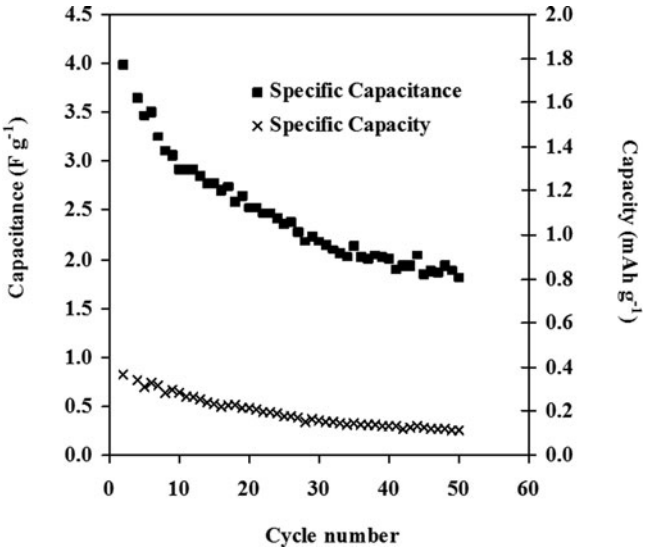

Figure 11. Specific capacitance and capacity versus cycle number.

to 0.85 V at a current density of 0.04 mA cm^{-2}. The EDLC shows typical charging and discharging performance, which is similar to that reported by Pandey et al. [56]. The curves are almost linear and further confirm the capacitive behavior of the EDLC [55, 56]. Figure 11 shows the calculated specific capacitance, (C_s) on selected cycles from the galvanostatic charge-discharge measurement using equation:

$$C_s = \frac{i}{m}\left(\frac{1}{s}\right) \tag{16}$$

where i is the constant current and s is the slope of the discharge curve. On the 50th cycle, the C_s is 1.82 F g^{-1}. The result shows higher C_s during the first 20 cycles which suggests that the material has potential for the use in EDLC [54]. Shuhaimi et al. [57] reported the discharge C_s for the EDLC cell with methyl cellulose-NH_4NO_3 polymer electrolyte is 1.67 F g^{-1}, which is close the C_s reported in this work. According to Sudhakar and Selvakumar [58], during the charging state, few ions still remain in the polymer matrix which significantly affects the charging and discharging process.

The specific capacity (Q) refers to the amount of charge passing through outer circuit during charge-discharge process per unit mass [54]. The values of Q were obtained from the following equation:

$$Q = \frac{t_d i}{m} \tag{17}$$

where t_d is the discharge time. The value of Q obtained is almost constant at ~0.15 mA h g^{-1} and shows the same trend as C_s as shown in Fig. 11. Shukur et al. [35] reported that the Q of EDLC using chitosan-PEO-NH_4NO_3-EC polymer electrolyte is ~0.01 mA h g^{-1}.

Conclusion

Starch-chitosan-NH_4I with different concentrations of glycerol were successfully prepared by the solution casting technique. FTIR analysis showed that the interaction occurred between the polymer host and the plasticizer. The highest room temperature conductivity was $(1.28 \pm 0.07) \times 10^{-3}$ S cm^{-1} with E_a value of 0.182, which obtained with the sample containing 30 wt% glycerol. Dielectric study suggests that the samples in this study show non-Debye behavior. The plot of conductivity-temperature proves that all electrolytes obeyed the Arrhenius rule. Employing the Rice and Roth model, the highest conducting sample (i.e. 30 wt% glycerol) had the highest n and μ values of 1.20×10^{19} cm^{-3} and 6.63×10^{-4} cm^2 V^{-1} s^{-1}, respectively. The conduction mechanism for the 30 wt% glycerol sample was best represented by the QMT model. In transference number analysis using the blocking electrode cell configuration, the total ionic transference number obtained was 0.991. LSV shows that this sample is electrochemically stable at 1.90 V. The EDLC shows specific capacitance values of 1.82–4.00 F g^{-1}.

Funding

The authors would like to thank the University of Malaya for the financial support provided (Grant No. RP010C-13AFR).

References

[1] Winie, T., Ramesh, S., & Arof, A. K. (2009). *Physica B*, *404*, 4308.
[2] Morni, N. M., Mohamed, N. S., & Arof, A. K. (1997). *Mater. Sci. Eng. B*, *45*, 140.
[3] Rozali, L. H., Samsudin, A. S., & Isa, M. I. N. (2012). *Int. J. Appl. Sci. Tech.*, *2*, 4.
[4] Ramly, K., Isa, M. I. N., & Khiar, A. S. A. (2011). *Mater. Res. Innov.*, *15*, S2–82.
[5] Kadir, M. F. Z., Aspanut, Z., Yahya, R., & and Arof, A. K. (2011). *Mater. Res. Innov.*, *15*, S2–164.
[6] Shukla, P. K., & Agrawal, S. L. (2000). *Ionics*, *6*, 312.
[7] Mohamed, N. S., Subban, R. H. Y., & Arof, A. K. (1995). *J. Power Sources*, *56*, 153.
[8] Schoenenberger, C., Le Nest, J. F., & Gandini, A. (1995). *Electrochim. Acta*, *40*, 2281.
[9] Morales, P. V., Le Nest, J. F., & Gandini, A. (1998). *Electrochim. Acta*, *43*, 1275.
[10] Zivanovic, S., Li, J., Davidson, P. M., & Kit, K. (2007). *Biomacromolecules*, *8*, 1505.
[11] Xu, Y., & Hanna, M. A. (2005). *J. Polym. Environ.*, *13*, 221.
[12] Tuhin, M. O., Rahman, N., Haque, M. E., Khan, R. A., Dafader, N. C., Islam, R., Nurnabi, M., & Tonny, W. (2012). *Radiat. Phys. Chem.*, *81*, 1659.
[13] Acosta, J. L., & Morales, E. (1996). *Solid State Ionics*, *85*, 85.
[14] Roberts, G. A. F. (1992). *Chitin Chemistry*, MacMillan Press, Ltd.: London.
[15] Sugimoto, M., Morimoto, M., Sashiwa, H., Saimoto, H., & Shigemasa, Y. (1998). *Carbohydr. Polym.*, *36*, 49.
[16] Crescenzi, V. (1994). *Trends Polym. Sci.*, *2*, 104.
[17] Burke, A., Yilmaz, E., Hasirci, N., & Yilmaz, O. (2002). *J. Appl. Polym. Sci.*, *84*, 1185.
[18] Luyen, D. V., & Huong, D. M. (1996). *Chitin and Derivatives*, Salamone, J. C. (Ed.), Polymeric Materials Encyclopedia, CRC Press: New York.
[19] Bourtoom, T., & Chinnan, M. S. (2008). *LWT–Food Sci. Tech.*, *41*, 1633.
[20] Zhai, M., Zhao, L., Yoshii, F., & Kume, T. (2004). *Carbohyd. Polym.*, *57*, 83.
[21] Mathew, S., & Abraham, T. E. (2008). *Food Hydrocolloid*, *22*, 826.
[22] Khiar, A. S. A., & Arof, A. K. (2010). *Ionics*, *16*, 123.
[23] Khiar, A. S. A., & Arof, A. K. (2011). *WASET*, *59*, 23.
[24] Buraidah, M. H., & Arof, A. K. (2011). *J. Non-Cryst. Solids*, *357*, 3261.
[25] Yusof, Y. M., Shukur, M. F., Illias, H. A., & Kadir, M. F. Z. (2014). *Phys. Scr.*, *89*, 035701.

[26] Liu, H., Adhikari, R., Guo, Q., & Adhikari, B. (2013). *J. Food Eng.*, *116*, 588.
[27] Vicentini, N., Dupuy, N., Leizelman, M., Cereda, M., & Sobral, P. (2005). *Spectrosc. Lett.*, *38*, 749.
[28] Bergo, P. V. A., Sobral, P. J. A., & Prison, J. M. (2009). *Gene Conserve*, *32*, 727.
[29] Shukur, M. F., Yusof, Y. M., Zawawi, S. M. M., Illias, H. A., & Kadir, M. F. Z. (2013). *Phys. Scr.*, *T157*, 014050.
[30] Buraidah, M. H., Teo, L. P., Majid, S. R., & Arof, A. K. (2009). *Physica B*, *404*, 1373.
[31] Ramesh, S., & Arof, A. K. (2001). *Mater. Sci. Eng. B*, *85*, 11.
[32] Woo, H. J., Majid, S. R., & Arof, A. K. (2012). *Mater. Chem. Phy.*, *134*, 755.
[33] Bhide, A., & Hariharan, K. (2007). *Eur. Polym. J.*, *43*, 4253.
[34] Sudhakar, Y. N., & Selvakumar, M. (2013). *J. Appl. Electrochem.*, *43*, 21.
[35] Shukur, M. F., Ithnin, R., Illias, H. A., & Kadir, M. F. Z. (2013). *Opt. Mater.*, *35*, 1834.
[36] Kadir, M. F. Z., Majid, S. R., & Arof, A. K. (2010). *Electrochim. Acta*, *55*, 1475.
[37] Rajendran, S., Sivakumar, M., & Subadevi, R. (2004). *Mater. Lett.*, *58*, 641.
[38] Majid, S. R., & Arof, A. K. (2005). *Physica B*, *355*, 78.
[39] Khiar, A. S. A., Puteh, R., & Arof, A. K. (2006). *Physica B*, *373*, 23.
[40] Rice, M. J., and Roth, W. L. (1972). *J. Solid State Chem.*, *4*, 294.
[41] Hashmi, S. A., Kumar, A., Maurya, K. K., & Chandra, S. (1990). *J. Phys. D: Appl. Phys.*, *23*, 1307.
[42] Shuhaimi, N. E. A., Teo, L. P., Majid, S. R., & Arof, A. K. (2010). *Synth. Met.*, *160*, 1040.
[43] Arof, A. K., Shuhaimi, N. E. A., Alias, N. A., Kufian, M. Z., & Majid, S. R. (2010). *J. Solid State Electrochem.*, *14*, 2145.
[44] Psarras, G. C., Manolakaki, E., & Tsangaris, G. M. (2003). *Composites Part A*, *34*, 1187.
[45] Murugaraj, R., Govindaraj, G., & George, D. (2003). *Mater. Lett.*, *57*, 1656.
[46] Kadir, M. F. Z. A., Teo, L. P., Majid, S. R., & Arof, A. K. (2009). *Mater. Res. Innov.*, *13*, 259.
[47] Matsuura, Y., Oshima, Y., Tanaka, K., & Yamabe, T. (1996). *Synth. Met.*, *79*, 7.
[48] Elkholy, M. M., & El-Mallawany, R. A. (1995). *Mater. Chem. Phys.*, *40*, 163.
[49] Majid, S. R., & Arof, A. K. (2007). *Physica B*, *390*, 209.
[50] Aziz, N. A., Majid, S. R., & Arof, A. K. (2012). *J. Non-Cryst. Solids*, *358*, 1581.
[51] Woo, H. J., Majid, S. R., & Arof, A. K. (2011). *Mater. Res. Innov.*, *15*, S2–49.
[52] Ng, L. S., & Mohamad, A. A. (2008). *J. Membr. Sci.*, *325*, 653.
[53] Kadir, M. F. Z., & Arof, A. K. (2011). *Mater. Res. Innov.*, *15*, S2–217.
[54] Arof, A. K., Kufian, M. Z., Syukur, M. F., Aziz, M. F., Abdelrahman, A. E., & Majid, S.R. (2012). *Electrochim. Acta*, *74*, 39.
[55] Lim, C. S., Teoh, K. H., Liew, C. W., & Ramesh, S. (2014). *Mater. Chem. Phys.*, *143*, 661.
[56] Pandey, G. P., Kumar, Y., & Hashmi S. A. (2011). *Solid State Ionics*, *190*, 93.
[57] Shuhaimi, N. E. A., S. R., & Arof, A. K. (2009). *Mater. Res. Innov.*, *13*, 171.
[58] Sudhakar, Y. N., & Selvakumar M. (2012). *Electrochim. Acta*, *78*, 398.